IAI Journals.ASM.org

Within-Host Selection Is Limited by an Effective Population of *Streptococcus pneumoniae* during Nasopharyngeal Colonization

Yuan Li,[a] Claudette M. Thompson,[a] Krzysztof Trzciński,[a,b] Marc Lipsitch[a]

Department of Epidemiology and Department of Immunology and Infectious Diseases, Harvard School of Public Health, Boston, Massachusetts, USA[a]; Department of Pediatric Immunology and Infectious Diseases, UMC Utrecht, Utrecht, The Netherlands[b]

***Streptococcus pneumoniae* (pneumococcus) is a significant pathogen that frequently colonizes the human nasopharynx. Environmental factors, including antimicrobial use and host immunity, exert selection on members of the nasopharyngeal population, and the dynamics of selection are influenced by the effective population size of the selected population, about which little is known. We measured here the variance effective population size (N_e) of pneumococcus in a mouse colonization model by monitoring the frequency change of two cocolonizing, competitively neutral pneumococcal strains over time. The point estimate of N_e during nasal carriage in 16 BALB/c mice was 133 (95% confidence interval [CI] = 11 to 203). In contrast, the lower-bound census population exhibited a mean of 5768 (95% CI = 2,515 to 9,021). Therefore, pneumococcal N_e during nasal carriage is substantially smaller than the census population. The N_e during day 1 to day 4 of colonization was comparable to the N_e during day 4 to day 8. Similarly, a low N_e was also evident for the colonization of pneumococcus in BALB/c mice exposed to cholera toxin 4 weeks prior to challenge and in another mouse strain (DO11.10 $RAG^{-/-}$). We developed a mathematical model of pneumococcal colonization composed of two subpopulations with differential contribution to future generations. By stochastic simulation, this model can reproduce the pattern of observed pneumococcal N_e and predicts that the selection coefficients may be difficult to measure *in vivo*. We hypothesized that such a small N_e may reduce the effectiveness of within host selection for pneumococcus.**

Studies of within-host competition between bacteria typically measure selection by the mean change in the logarithm of the ratio of a favored to a disfavored allele (1–4), sometimes called a "competitive index." In animal experiments, there is often substantial variation in the competition outcome among animal subjects (1–4), which necessitates the use of a large number of animals to ensure reproducible results (5). Understanding the source of this variation is important for a number of purposes, including sample size calculations in experimental design and results interpretation. For example, modern methods for identifying genes important for fitness in certain environments, such as transposon mutagenesis screens, rely on the ability of many members of a large inoculum to establish infection, so that variations in mutant frequency may be attributed to selection rather than chance. From the opposite perspective, predictions of quantitative models of selection within a host for immune escape or emergence of resistant variants depend not only on the strength of selection but also on the number of pathogen individuals available for selection (3, 6, 7).

The variation in competitive index in experiments is rarely commented on, as if the presence of noise in results was an inevitable consequence of animal experiments. Stochasticity introduced by population bottlenecks and by small effective population size can also contribute to the observed variation. Since the first transposon mutagenesis study that relied on interpretation of allele frequency change to infer fitness effects of gene knockouts (8), this has been an important issue that needs to be accounted for implicitly or explicitly (9). In population genetics, stochasticity in the fate of alleles under selection (as well as that of neutral alleles) is explained by the concept of effective population size, which intuitively is related to the number of individuals in each generation who contribute to the next (10), making allowance for the fact that contributions may be uneven for many reasons. More precisely, the effective size of a population (N_e) is defined by the value that produces an observed distribution of changes in the frequencies of unselected alleles due to stochasticity in the reproduction of a finite population and can be estimated from this distribution, with a larger N_e corresponding to smaller stochastic fluctuations (10). N_e is an important parameter in understanding the dynamics of population diversity since it controls, among other genetic processes, the effectiveness of selection relative to genetic drift. A small N_e increases the relative weight of genetic drift over selection in determining allele frequency, so that the difference between the chance of fixing a favorable mutation and the chance of fixing a neutral mutation in the population is reduced (10). Because bacterial pathogens usually show large census populations (i.e., the number of CFU per host), many experiments have been performed with the assumption that the median or mean change in frequency of one variant compared to another is a good representation of the selective value of those variants *in vivo* (1, 2, 11–15), although researchers may make allowance for the noise involved when small numbers of each variant are present in a small population, such as in transposon-mutant screens (13). Although little is known about the actual N_e of bacterial populations within individual hosts, it is possible that N_e is smaller than the census population because of the observed subpopulation

Received 8 August 2013 **Returned for modification** 5 September 2013
Accepted 22 September 2013
Published ahead of print 30 September 2013
Editor: A. Camilli
Address correspondence to Yuan Li, liyuan@hsph.harvard.edu.
Supplemental material for this article may be found at http://dx.doi.org/10.1128/IAI.00527-13.

doi:10.1128/IAI.00527-13

structure (16), which may lead to heterogeneity in the reproductive potential of members of the population. We therefore hypothesize that limited effective population sizes contribute to the variability of competition outcome when the sizes are small enough to make even a fully neutral marker drift significantly.

Streptococcus pneumoniae (pneumococcus) is an important pathogen that frequently colonizes the human nasopharynx. Although nasopharyngeal colonization is usually asymptomatic, it is a critical step prior to invasive infections (17, 18). The nasopharyngeal carriage population serves as a reservoir of bacteria that may be transmitted to other hosts. In humans, an average carrier harbors at least 10^3 to 10^5 pneumococci (19), and the duration of colonization ranges from 1 week to several months (19). More importantly, most transmission of pneumococci occurs from healthy carriers, making the nasopharyngeal colonization a key stage in the evolution and ecology of these organisms. The effect of selection pressures imposed by host immunity, competition with other microflora, and antimicrobial treatment will depend on the effective population size. This is both because a small N_e limits the amount of genetic variation (i.e., mutations and recombination events) available for selection and because, in simple population-genetic models, selection can be effective only if the product of the selection coefficient and N_e is substantially greater than 1; otherwise, selection will typically be overwhelmed by genetic drift. An understanding of within host N_e would be valuable in understanding the population dynamics of pneumococcus *in vivo*.

We assessed here how much stochastic effects influence the outcome of animal experiments by measuring the N_e of pneumococcus in a mouse colonization model and modeling its effects on within-host selection. We found that N_e was substantially smaller than the carriage population size. It appeared that N_e did not change over time during colonization. Simulation studies suggested that such a small N_e could reduce the efficiency of within-host selection for favored variants.

MATERIALS AND METHODS

Strains and animals. The OVA and AVO stains were serotype 6B pneumococcal strain 603 derivatives that were described previously (3). Briefly, these were derivatives of clinical strain 603 with either OVA323-339 peptide (ISQAVHAAHAEINEAGR) or the reverse "AVO" peptide (RGAEN IEAHAAHVAQSI) fused with two pneumococcal proteins: pneumococcal surface protein A (PspA) and pneumolysin (Ply). Wild-type BALB/c (BALB/c) mice and BALB/c DO11.10 $RAG^{-/-}$ (DO11.10) mice were obtained from the Jackson ImmunoResearch Laboratories, Bar Harbor, ME. All mice were female, 9 to 10 weeks old at the start of experiments, and kept in a BL2 facility. Some mice were intranasally administered 1 μg of cholera toxin (CT; List Biological Laboratories, Compel, CA) 4 or 5 weeks prior to challenge, because these mice were controls in other experiments in which the experimental mice received immunizations using CT as an adjuvant. The data analyzed in the present study are a combination of newly generated data (BALB/c and DO11.10 $RAG^{-/-}$ mice) and the frequencies from controls in experiments previously published for the BALB/c mice with CT (3). The mouse experiment protocols were approved by Institutional Animal Care and Use Committee of Harvard University.

Mouse carriage model and strain quantification. BALB/c or DO11.10 $RAG^{-/-}$ mice were inoculated intranasally with a mix of the OVA and the AVO strains in 10 μl of phosphate-buffered saline containing approximately 5×10^6 CFU of each strain. Nasal wash samples were collected up to 8 days after challenge according to a method described previously (3). Aliquots of each sample were titered to determine the CFU density in sample. The remaining samples were cultured overnight on blood agar plates supplemented with gentamicin to a final concentration of 2.5 mg/liter, and all bacterial growth was harvested for genomic DNA extraction.

TABLE 1 CFU counts used for N_e estimation in the BALB/c mouse experiment

Mouse	CFU count					
	Day 1		Day 4		Day 8	
	AVO	OVA	AVO	OVA	AVO	OVA
1-1	1,510	2,468	877	971	643	233
1-2	8	2	170	76	67	72
1-3	200	249	34	233	386	3,163
1-4	378	370	52	364	9	12
1-5	4,432	8,623	676	8,248	2,472	7,582
2-2	1,099	1,750	387	1,098	292	477
2-3	22	42	77	115	759	1,378
3-1	57	28	117	65	288	0
3-2	1,948	3,858	1,328	2,651	2,316	19,628
3-3	3,107	2,484	1,124	1,241	4,448	6,896
3-4	2,092	4,413	530	891	1,980	2,429
3-5	283	294	150	95	10,254	5,579
4-1	31	33	70	58	70	90
4-3	848	765	523	1,896	1,880	5,055
4-4	1,775	1,988	247	234	765	1,171
4-5	95	97	7	15	657	1,440

Genomic DNA was purified from cultures of samples collected from animals using a DNeasy blood and tissue kit (Qiagen, Valencia, CA). OVA strain- and AVO strain-specific primer sets were designed based on the nucleotide sequence difference in the *pspA* locus between the two strains. The quantity of strain-specific genomic DNA in a sample was determined by real-time PCR as described previously (3). The AVO/OVA ratio for each sample was calculated by using the absolute amount of OVA DNA and AVO DNA in the sample. The CFU counts for AVO and OVA bacteria in a sample were estimated from the total CFU and the AVO/OVA ratio (Table 1).

Bacterial growth curve. AVO and OVA strains were streaked onto blood agar plates and cultured at 37°C in a 5% CO_2 overnight. Four colonies from each strain were subcultured in Todd-Hewitt medium with 0.5% yeast extract (THY; Becton Dickinson, Sparks, MD) until the optical density at 620 nm (OD_{620}) reached ~0.4 and then diluted into THY medium at a starting culture OD_{620} of ~0.005. Growth was monitored in sterile flat-bottom 96-well microtiter plates (Nunc, Denmark) containing 200 μl of culture in each well every 30 min using a VERSAmax microplate reader (Molecular Devices, Sunnyvale, CA) over 6 h. The growth curves were fitted to an exponential growth equation, and the doubling time was estimated using Prism software (GraphPad Software, Inc., La Jolla, CA).

Estimation of variance effective population (N_e). MLNE software (20, 21) was used to estimate the maximum-likelihood N_e and its 95% confidence interval (CI). Essentially, the software uses the probability of observing the CFU count data (Table 1) in a sample at a given time as a function of the CFU count data in a previous sample, the number of generations during the sampling period, and the (harmonic) mean effective size (N_e) of the population (22). The estimation procedure in MLNE function further accounted for the probability of observing the CFU count data in a sample given a true ratio between the two strains in the underlying population and thus explicitly accounted for sampling error caused by examining the allelic composition of a finite number of bacterial CFU. When the CFU count data in all time points are given, the software will maximize the likelihood of the data by varying the N_e. We assumed that N_e was the same for each mouse, and the frequency of AVO and OVA bacteria in different mice at each time point in a single experiment could be treated as if they were alleles at independently assorting loci. The likelihood maximized by the software in this way corresponds to

the assumption that N_e was the same in each mouse, so each mouse contributes independent data to the estimation of that single quantity. To estimate the pneumococcal N_e during colonization in BALB/c mice, the CFU count data on days 1, 4, and 8 were used. To estimate the average pneumococcal N_e during colonization in DO11.10 RAG$^{-/-}$ mice, the CFU count data on days 1, 3, and 7 were used. Allele frequency change from the time of inoculation (day 0) to day 1 was not considered in N_e estimation to minimize the effect of colonization bottleneck. Any mouse with missing data on any of the three sampling time points was also excluded from analysis. The input data for MLNE were prepared according to software instructions with each mouse replicate being treated as an independent locus. The number of pneumococcal generations between two sampling time points was calculated by dividing the length of time between two samplings by the average life span of pneumococcus. We used (cells doubling time)/ln (2) as the average life span according to a simple exponential-growth/exponential-death model at its equilibrium. Due to the haploidy of pneumococcal genome, the N_e and 95% CI estimated by the MLNE software (designed for diploids) were scaled up by a factor of 2 (Jinliang Wang, unpublished data), a scaling that we validated by preliminary simulation (data not shown).

Simulation of pneumococcal colonization population. A simple model of heterogeneity in bacterial reproduction that could generate a small effective population size is one similar to that described by Balaban et al. (23) for "type 1 persisters." This model represents the pneumococcal colonization population as composed of two subpopulations, P_1 and P_2. P_1 is a small subpopulation that actively replicates, while P_2 represents a large subpopulation where most bacterial death/removal occurs. Each subpopulation is composed of two strains, A and O, that satisfy $P_1 \equiv A_1 + O_1$ and $P_2 \equiv A_2 + O_2$. The dynamics of A_1, O_1, A_2, and O_2 is described by equations 1 to 4:

$$\frac{dA_1}{dt} = \mu A_1 - \frac{\mu A_1(A_1 + O_1)}{K_1} - d_a A_1 \quad (1)$$

$$\frac{dO_1}{dt} = \mu O_1 - \frac{\mu O_1(A_1 + O_1)}{K_1} - d_o O_1 \quad (2)$$

$$\frac{dA_2}{dt} = \frac{\mu A_1(A_1 + O_1)}{K_1} + \mu A_2\left(1 - \frac{A_2 + O_2}{K_2}\right) - d_a A_2 \quad (3)$$

$$\frac{dO_2}{dt} = \frac{\mu O_1(A_1 + O_1)}{K_1} + \mu O_2\left(1 - \frac{A_2 + O_2}{K_2}\right) - d_a O_2 \quad (4)$$

For competitively neutral strains to achieve stable carriage, we assumed that $d_a = d_o = d$ and that $\mu > d$. Essentially, strains in P_1 follow exponential growth and clearance, with the probability of the descendant cell's remaining in P_1 decreasing with the number of cells in P_1; otherwise, it migrates to P_2 (equations 5 and 6), with the migration modeled as a separate event. Strains in P_2 grow logistically and are also subjected to exponential clearance.

$$\frac{dP_1}{dt} = \mu P_1 - \frac{\mu P_1^2}{K_1} - dP_1 \quad (5)$$

$$\frac{dP_2}{dt} = \frac{\mu P_1^2}{K_1} + \mu P_2\left(1 - \frac{P_2}{K_2}\right) - dP_2 \quad (6)$$

Equation 5 combines equations 1 and 2; equation 6 combines equations 3 and 4. The stable equilibrium subpopulation size of P_1 and P_2 is given by:

$$P_1^* = A_1^* + O_1^* = \frac{\mu - d}{\mu}K_1 \quad (7)$$

$$P_2^* = A_2^* + O_2^* = \frac{(\mu - d)(1 + \sqrt{1 + \frac{1 + 4K_1}{K_2}}}{2\mu}K_2 \quad (8)$$

Note that when growth is blocked ($\mu = 0$), the total population ($P_1 + P_2$) follows an exponential decay: $d(P_1 + P_2)/dt = -d(P_1 + P_2)$. In this situation, the half-life ($\ln_2/d$) of pneumococcus during mouse nasal colonization has been estimated to be 161 min (13). Unless otherwise specified, the clearance rate $d = 0.0043$ min^{-1} ($\ln_2/161$ min^{-1}) and the maximum growth rate $\mu = 0.0231$ min^{-1} were used. Varied K_1 and K_2 values were used as indicated.

TABLE 2 Transition rates for simulation of the colonization population

Event	Effects (A_1, O_1, A_2, O_2)	Transition rate (0)[a]
Birth		
A_1	1, 0, 0, 0	μA_1
O_1	0, 1, 0, 0	μO_1
Migration		
A_1	–1, 0, 1, 0	$\mu A_1 (A_1 + O_1)/K_1$
O_1	0, –1, 0, 1	$\mu O_1 (A_1 + O_1)/K_1$
Clearance		
A_1	–1, 0, 0, 0	$d_a A_1$
O_1	0, 1, 0, 0	$d_o O_1$
Birth		
A_2	0, 0, 1, 0	Max {0, $\mu A_2 [1 – (A_2 + O_2)/K_2]$}
O_2	0, 0, 0, 1	Max {0, $\mu A_2 [1 – (A_2 + O_2)/K_2]$}
Death		
A_2	0, 0, –1, 0	–Min {0, $\mu A_2 [1 – (A_2 + O_2)/K_2]$}
O_2	0, 0, 0, –1	–Min {0, $\mu O_2 [1 – (A_2 + O_2)/K_2]$}
Clearance		
A_2	0, 0, –1, 0	$d_a A_2$
O_2	0, 0, 0, –1	$d_o O_2$

[a] Max, function that returns the largest value of the input values; min, function that returns the smallest value of the input values.

Our simulation was a stochastic version of the model described by equations 1 to 4. To generate simulation data of allele frequency, we used the "adaptivetau" package in R (24), which implements an adaptive tau leaping to approximate the trajectory of a continuous-time stochastic process. The instantaneous transition rate for each transition and its effects are given in Table 2.

To initialize the simulation, $A_1 + O_1$ and $A_2 + O_2$ were first set to their equilibrium size (P_1^* and P_2^* in equations 7 and 8, respectively). To mimic the allele frequency distribution on day 1 of colonization, a value of $\log_{10}(a)$ was randomly drawn from a normal distribution estimated from the BALB/c colonization experiment (equation 9), where a is the ratio between the two strains in each subpopulation ($a \equiv A_i/O_i$, i = 1,2). The specific initial state (A_1, O_1, A_2, and O_2) was then calculated according to the value of a and equations 10 to 13.

$$\log_{10} a \sim N(0, 0.23^2) \quad (9)$$

On day 1:

$$A_1 = P_1^* \frac{a}{1 + a} \quad (10)$$

$$O_1 = P_1^* \frac{1}{1 + a} \quad (11)$$

$$A_2 = P_2^* \frac{a}{1 - a} \quad (12)$$

$$O_2 = P_2^* \frac{a}{1 - a} \quad (13)$$

After initiation, the model was first simulated forward for $t = 4{,}320$ min (3 days) by using the "ssa.adaptivetau" function in the "adaptivetau" R package (24). The values of A_1, O_1, A_2, and O_2 at the end of the $t = 4{,}320$ min were recorded as the day 4 output. Continuing from this state, the model

was subsequently simulated forward for another 5,760 min (4 days), and the end values of A_1, O_1, A_2, and O_2 were recorded as the day 8 output.

The N_e of the simulated population was estimated by the MLNE software using a method similar to what is described in the previous section. Briefly, the values of A_2 and O_2 on days 1, 4, and 8 of simulation were used as allele count data in the input file of the MLNE software. Twenty replicate simulations were performed for any given set of parameters (μ, d, K_1, and K_2). The values of A_2 or O_2 on days 1, 4, and 8 in each replicate simulation were used as allele counts from an independent locus in the input file of the MLNE software. As for the experimental data, the N_e and 95% CI estimated by the MLNE software were scaled up by a factor of 2. To estimate the N_e of the simulated population between days 1 and 4, values of A_2 and O_2 on days 1 and 4 in each replicate simulation were used. Similarly, the values of A_2 and O_2 on days 4 and 8 in each replicate simulation were used to estimate the N_e of the simulated population between days 4 and 8.

Simulation of within-host selection in the colonizing population. To examine the influence of N_e on the efficiency of within host selection, the pneumococcal colonization model was modified to incorporate selection mediated by different clearance rates for a wild-type strain (O) and a mutant strain (A) (i.e., $d_a \neq d_o$); otherwise, the equations are the same as equations 1 to 4 and Table 2. The parameters used in the simulation were $\mu = 0.0231\ \text{min}^{-1}$, $d_o = 0.0043\ \text{min}^{-1}$, $K_1 = 400$, and $K_2 = 40{,}000$, which corresponded to an estimated N_e of 181 according to previous simulations. Varied d_a values were used as indicated.

To initialize the simulation, $A_1 + O_1$ and $A_2 + O_2$ were first set to the carrying capacities (400 and 40,000, respectively). The specific values of A_1, O_1, A_2, and O_2 were then set to satisfy that $A_1/O_1 = A_2/O_2 = a$, where a is a given initial ratio between mutant and wild-type alleles. After initiation, the model was first simulated forward for $t = 5{,}760$ min (4 days). The value of A_1, O_1, A_2, or O_2 at the end of the $t = 5{,}760$ min was recorded as the day 4 output. Continuing from this state, the model was subsequently simulated forward for another 5,760 min (4 days), and the end value of A_1, O_1, A_2, or O_2 was recorded as the day 8 output. The A_2 and O_2 outputs on days 4 and 8 of simulation were used to calculate the mutant allele frequency $[A_2/(A_2 + O_2)]$. Twenty replicate simulations were performed. The average census population size $(A_2 + O_2)$ during the simulation was approximately 33,000.

Simulation of within-host selection by an ideal population model. The ideal population is a single population with a wild-type strain (O) and a mutant strain (A) undergoing selection mediated by different clearance rates (equations 14 and 15). The parameters used in simulation were $\mu = 0.0231\ \text{min}^{-1}$, $d_o = 0.0043\ \text{min}^{-1}$, and $K = 40{,}000$. Varied d_a values were used as indicated.

The following equations express the ideal population model:

$$\frac{dA}{dt} = \mu A\left(1 - \frac{A + O}{K}\right) - d_a A \tag{14}$$

$$\frac{dO}{dt} = \mu O\left(1 - \frac{A + O}{K}\right) - d_o O \tag{15}$$

Simulation data of allele frequency were generated by using the "adaptivetau" package in R (24), and the instantaneous transition rates are listed in Table 3. To initialize the simulation, $A + O$ was first set to the carrying capacity (40,000). The specific values of A and O were then set to satisfy that $A/O = a$, where a is a given initial ratio between mutant and wild-type alleles. After initiation, the model was first simulated forward for $t = 5{,}760$ min (4 days). The value of A or O at the end of the $t = 5{,}760$ min was recorded as the day 4 output. Continuing from this state, the model was subsequently simulated forward for another 5760 min (4 days) and the end value of A or O was recorded as the day 8 output. The A and O outputs on days 4 and 8 of simulation were used to calculate the mutant allele frequency $[A/(A + O)]$. Twenty replicate simulations were performed. The average census population size $(A + O)$ during simulation was approximately 32,000.

TABLE 3 Transition rates for simulation of the ideal population

Event	Effects (A, O)	Transition rate (≥ 0)[a]
Birth		
A	1, 0	Max $\{0, \mu A_2\,[1 - (A + O)/K]\}$
O	0, 1	Max $\{0, \mu A_2\,[1 - (A + O)/K]\}$
Death		
A	−1, 0	−Min $\{0, \mu A_2\,[1 - (A + O)/K]\}$
O	0, −1	−Min $\{0, \mu O_2\,[1 - (A + O)/K]\}$
Clearance		
A	−1, 0	$d_a A$
O	0, −1	$d_o O$

[a] Max, function that returns the largest value of the input values; min, function that returns the smallest value of the input values.

Statistical analysis was performed by using the R package (http://CRAN.R-project.org/) and the GraphPad Prism software.

RESULTS

Pneumococcal variants showed genetic drift during nasal colonization. To investigate the effective population size of pneumococcus during nasal carriage, we used two competitively neutral strains, the AVO strain and the OVA strain, which have been described previously (3). The two strains showed similar *in vitro* growth rates in THY medium (Fig. 1A). The average doubling time of the AVO strain (62 min, 95% CI = 55 to 70) was not significantly different from that of the OVA strain (65 min, 95% CI = 57 to 76) (Fig. 1A, Student t test, $P = 0.82$).

To quantify genetic drift *in vivo*, 20 BALB/c mice were intranasally challenged by a 1:1 mixture of the AVO and OVA strains. We measured the total CFU and the AVO/OVA ratio in the nasal washes as described in Materials and Methods. The mean $\log_{10}$(AVO/OVA) values were 0.067 ($n = 20$, standard deviation [SD] = 0.23), −0.014 ($n = 16$, SD = 0.76), and 0.070 ($n = 19$ SD = 1.04) on days 1, 4, and 8, respectively (Fig. 1B). None of the mean $\log_{10}$(AVO/OVA) values were significantly different from the input $\log_{10}$(AVO/OVA) ($P > 0.05$, one sample t test). In contrast, the variance of $\log_{10}$(AVO/OVA) showed a significant increase over time (Fig. 1B, Levene's test for equal variance, $P = 0.034$). Furthermore, no significant correlation between change in AVO/OVA from day 0 to day 1 and change from day 4 to day 8 was observed (Fig. 1C, $n = 16$, rho = 0.20, $P = 0.45$). In similar colonization experiments carried out in BALB/c mice exposed to immunization adjuvant (cholera toxin) 4 weeks prior to challenge, no correlation between change in AVO/OVA from day 0 to day 1 and change from day 4 to day 8 was observed either (Fig. 1D, $n = 9$, rho = −0.38, $P = 0.31$). The lack of consistent AVO/OVA ratio change in an individual mouse argued against selection for heritable fitness differences acquired by a subpopulation of one of the strains during nasal colonization.

Estimation of effective population size. Based on the temporal change of AVO strain frequency in each mouse, we estimated N_e by using the MLNE software (25), which implements a maximum-likelihood method and accounts for sampling error. An *in vivo* doubling time of 161 min (13) was assumed to estimate the number of generations between two sampling points. In BALB/c mice, the effective population of pneumococcus showed a point estimate of 133 with 95% CI of 11 to 203 (Fig. 2A). In comparison, the CFU recovered on day 8 showed a mean of 5,768 with a 95%

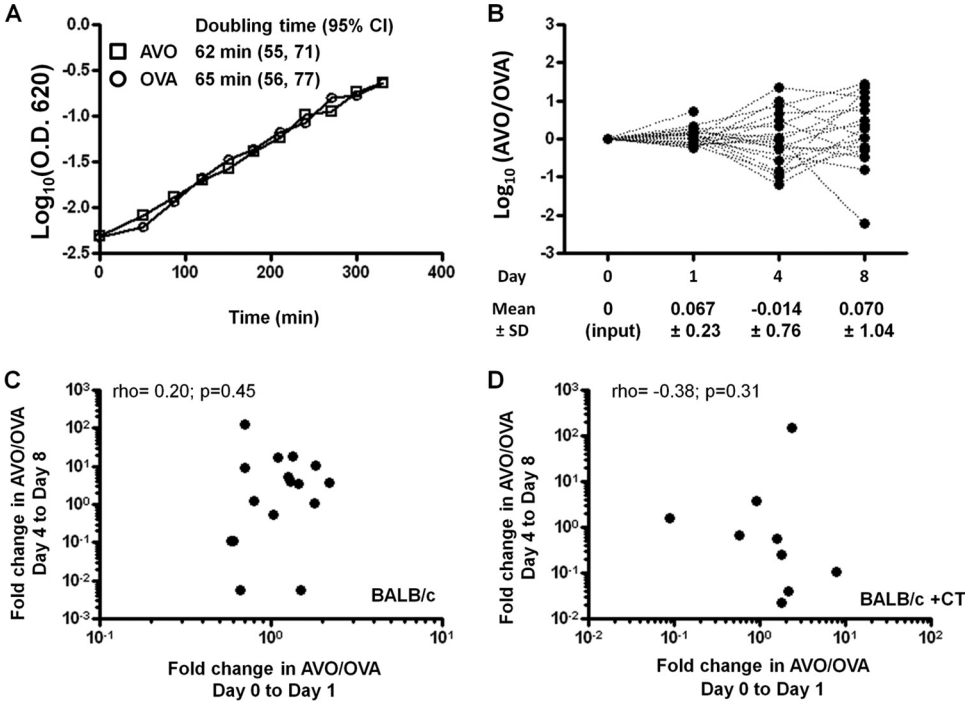

FIG 1 AVO and OVA are neutral alleles and show genetic drift during nasal carriage. (A) The AVO and OVA strains were cultured in THY medium at 37°C, and the increase in OD_{620} was measured every 30 min. The curve was fitted to an exponential growth to estimate the average doubling time. (B) Twenty BALB/c mice were intranasally challenged by a 1:1 mixture of the AVO and OVA strains (day 0). The AVO/OVA ratio in mouse nasal wash was measured on days 1, 4, and 8. Each dashed line connects points for the same mouse over time. (C) Scatter plots to examine correlation between the change in AVO/OVA from day 0 to day 1 and the change in AVO/OVA from day 4 to day 8 in BALB/c mice. (D) Scatter plots to examine correlation between the change in AVO/OVA from day 0 to day 1 and the change in AVO/OVA from day 4 to day 8 in BALB/c mice who had been treated with cholera toxin (CT) 4 weeks prior to challenge.

confidence interval of 2,515 to 9,021 (Fig. 2A). Since CFU recovered on day 8 represents only a fraction of the carriage population, we concluded that the N_e of pneumococcus is much smaller than the carriage population during nasal colonization.

A number of *in vitro* studies indicated that the doubling time of pneumococcus could be much shorter than 161 min (13, 26). We therefore tested whether a shorter generation time could explain the discrepancy between carriage population and effective popu-

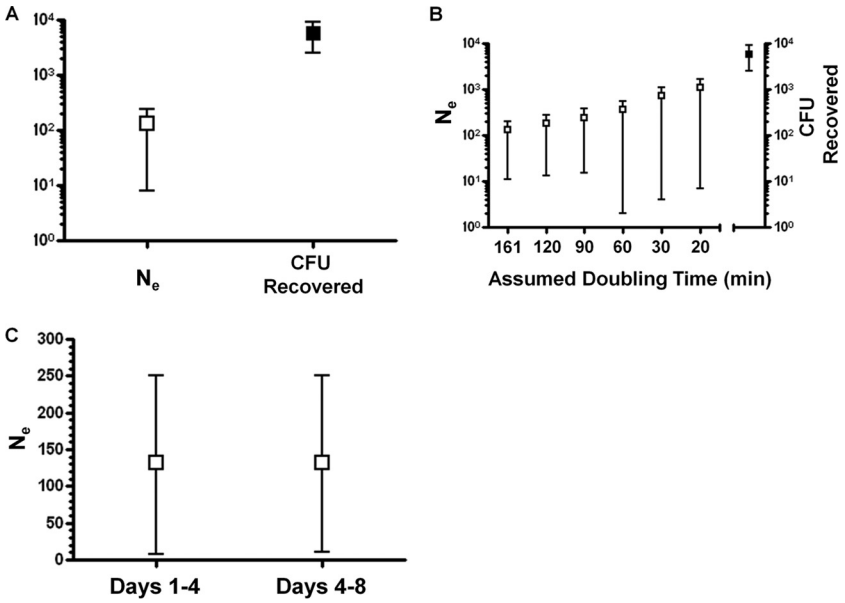

FIG 2 Effective population of pneumococcus in BALB/c mice. (A) The estimated N_e in BALB/c mice (□) was lower than the CFU recovered on day 8 (■). (B) A range of *in vivo* generation time was assumed, and the estimated N_e values (left panel) were compared to the CFU recovered on day 8 (right panel). (C) The N_e for different time intervals was estimated by only using the strain frequency data during the time period specified. Error bars represent the 95% CI.

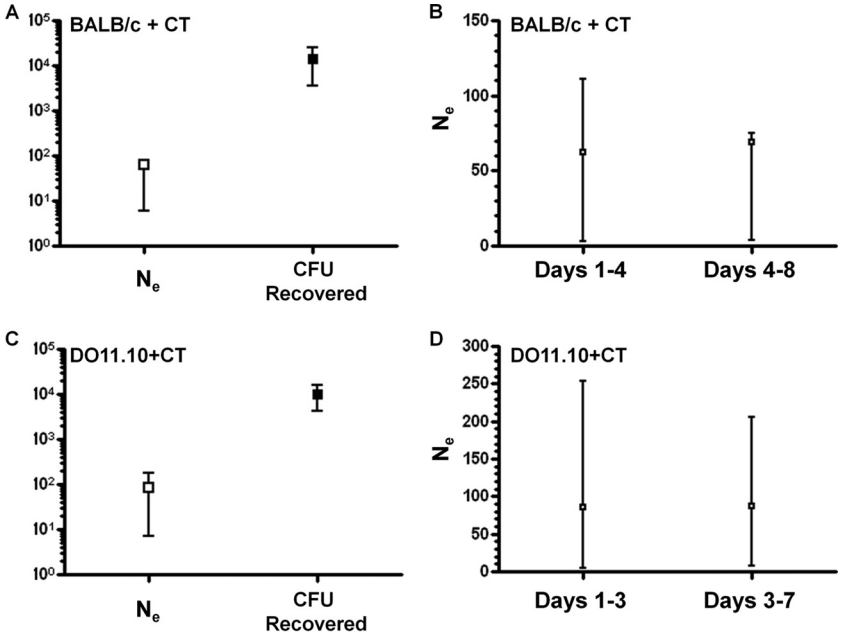

FIG 3 Effective population of pneumococcus in BALB/c and DO11.10 RAG$^{-/-}$ mice. All mice had been exposed to CT 4 to 5 weeks prior to challenge. The point estimate of N_e (□) and mean CFU recovered (■) are shown. The estimated N_e in BALB/c mice (A) or DO11.10 RAG$^{-/-}$ mice (C) was lower than the terminally recovered CFU. The N_e in different time intervals was calculated by only using the strain frequency data during the time period specified in BALB/c mice (B) and DO11.10 RAG$^{-/-}$ mice (D). Error bars represent the 95% CI.

lation. A range of generation times was assumed and the corresponding effective population size was calculated (Fig. 2B). As expected, effective population size increased when generation time became shorter (Fig. 2B). However, the effective population size was still substantially smaller than the CFU recovered even an unrealistically short generation time (20 min) was assumed (Fig. 2B). Thus, a short generation time *in vivo* was unlikely to be the major explanation for the small N_e.

We next examined whether there is temporal change in pneumococcal N_e during colonization. The average N_e from day 1 to day 4 (days 1 to 4) was calculated by using the AVO allele frequency change between day 1 and day 4. The same strategy was used to estimate average N_e during days 4 to 8. As shown in Fig. 2C, the estimation of N_e for days 1 to 4 (point estimate, 132; 95% CI = 7 to 250) was very similar to the estimation of N_e for days 4 to 8 (point estimate, 132; 95% CI = 11 to 250). The N_e estimated for the two time intervals were much lower than the CFU recovered on day 8, a finding consistent with the overall N_e.

Finally, the effective population size of pneumococcus during nasal carriage in varied experimental conditions, as well as in a different mouse type, was investigated. Cholera toxin (CT) is a commonly used adjuvant in immunization experiments, and here we examined its effect on N_e in BALB/c mice. In BALB/c mice exposed to CT (BALB/c + CT), the effective population of pneumococcus showed point estimate of 64 (95% CI = 6 to 65) (Fig. 3A, $n = 8$). Similar to what was observed in naive BALB/c mice, the N_e was substantially smaller than the CFU recovered on day 8 (mean, 14,641; 95% CI = 3,620 to 25,655) (Fig. 3A). The estimation of N_e for days 1 to 4 (point estimate, 62; 95% CI = 3 to 111) was similar to the estimation of N_e for days 4 to 8 (point estimate, 69; 95% CI = 4 to 75) (Fig. 3B). It appeared that exposure to CT reduced pneumococcal N_e in BALB/c mice.

In DO11.10 RAG$^{-/-}$ mice (which lack adaptive B cell and T cell immunity, except for CD4$^+$ T cells specific for a peptide of ovalbumin) exposed to CT (DO11.10 + CT), the effective population of pneumococcus showed point estimate of 87 (95% CI = 7 to 181) (Fig. 3C, $n = 7$). Again, the N_e was much smaller than the CFU recovered on day 8 (mean, 9,931; 95% CI = 4,155 to 15,708) (Fig. 3C). The estimation of N_e for days 1 to 3 (point estimate, 86; 95% CI = 5 to 245) was similar to the estimation of N_e for days 3 to 7 (point estimate, 87; 95% CI = 7 to 206) (Fig. 3D). Thus, the N_e of pneumococcus in DO11.10 RAG$^{-/-}$ mice showed qualitatively similar patterns as in BALB/c mice.

A mathematical model reproduced the N_e patterns. The large discrepancy between N_e and carriage census population size would be most readily explained by heterogeneity in pneumococcal replication during nasopharyngeal colonization. Indeed, the nasal mucosa may support two populations of pneumococci, which can be primarily recovered from the outer surface and the nasal tissue, respectively (16). To examine whether the heterogeneous nasal environment can explain the observed N_e patterns, we modeled pneumococcal colonization by considering two subpopulations, P_1 and P_2 that are established 1 day after inoculation (Fig. 4A). Loosely based on the idea of the type I persister described by Balaban et al. (23), we hypothesized that a small subpopulation of pneumococci (P_1), perhaps tissue associated (16), actively replicates, while a larger population that is in the nasopharyngeal lumen or mucosal surface (P_2) may or may not replicate but does not contribute to the future generations which are seeded by the P_1 population. Effectively, P_2 is the major site of bacterial death and removal. Note that this is a deliberate simplification, in the absence of detailed information concerning the heterogeneity in dynamics of the colonizing population over time.

We simulated this model, tracking OVA and AVO strains sep-

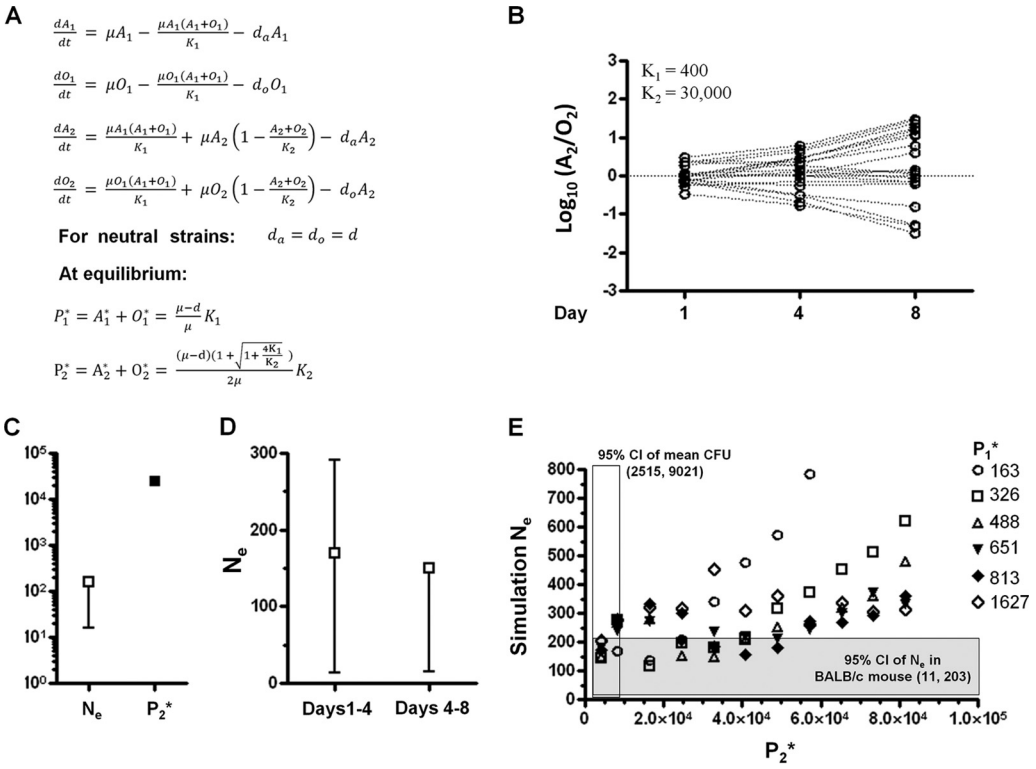

FIG 4 Mathematical model of pneumococcal colonization dynamics. (A) Differential equations describing the dynamics of two strains (A and O) in two subpopulations, P_1 and P_2. A stochastic version of this model was used in simulation. To initialize the simulation, P_1 and P_2 were set to their equilibrium size (P_1* and P_2*, respectively), and the ratio between the two strains in each subpopulation was set to follow a log-normal distribution as estimated from the day 1 results of the BALB/c colonization experiment. After initiation, the model was simulated forward for a total of $t = 10{,}080$ min (7 days), and the counts of the two strains in each subpopulation on days 1, 4, and 8 were recorded as output. (B) Typical results from 20 simulations with the indicated parameter values. The $\log_{10}(A_2/O_2)$ calculated from the simulation output is shown, and each dashed line connects data points from the same simulation. (C) Simulation of the model produced small N_e despite large census population size. The point estimate of N_e (□) calculated from output of 20 simulations in panel B is shown, which is substantially smaller than the census population size P_2* (■) used in the simulation. Error bars indicate the 95% CI. (D) Simulation of the model showed little temporal change in N_e. N_e was calculated from output of 20 simulations shown in panel B and the N_e in different time intervals was estimated by only using the strain frequency data during the time period specified. Error bars indicate the 95% CI. (E) Effects of P_1* and P_2* size on the estimated N_e. Simulation was performed with varying K_1 and K_2 values such that the indicated P_1* and P_2* sizes were achieved. Twenty simulations were performed for each combination of P_1* and P_2*, and the point estimate of N_e based on that 20 simulation output is shown. The shaded area represents where the simulated N_e values fall within the 95% CI of N_e estimated from the BALB/c colonization experiment, and the census population size used in the simulation (P_2*) is no smaller than the census population size observed in the BALB/c colonization experiment (95% CI of mean CFU recovered, open bar).

arately, in a continuous-time stochastic process. Typical results of 20 simulation outputs for a particular parameter combination ($K_1 = 400$, $K_2 = 30000$) are shown in Fig. 4B. N_e was estimated based on the simulated outputs and compared to the equilibrium size of P_2, which was treated as the census population since it represents the vast majority of $P_1 + P_2$ in our simulation. As shown in Fig. 4C, the N_e estimated from the simulation outputs (163; 95% CI = 16 to 174) was similar to the N_e estimated for pneumococcus in BALB/c mice and was much smaller than the equilibrium size of P_2 (24737) that was used to generate the simulation outputs. For the simulated data, the estimation of N_e for days 1 to 4 (point estimate, 169; 95% CI = 14 to 291) was also similar to the estimation of N_e for days 4 to 8 (point estimate, 150; 95% CI = 15 to 151) (Fig. 4D). In addition, we estimated N_e based on simulation data generated from varied K_1 and K_2 to examine effects of census population (P_2*) on N_e (Fig. 4E). We found that a wide range of simulation census population ([4,226 to 48,993], Fig. 4E) that was consistent with the observed CFU recovered can generate similar N_e to those observed in the BALB/c mice experiment.

Facilitated by the pneumococcal colonization model, we further investigated the pattern of allele frequency change in the colonizing population when the clearance rate of the A strain bacteria is different from that of the O strain bacteria, as might be the case of under selection for escape from strain-specific immune responses or antimicrobial agents. The results were compared to those from an ideal population in which the census size and effective size are nearly equal (Fig. 5). In both populations, the census size was approximately 30,000 during simulation. Selection would be expected to operate efficiently down to a selection coefficient of order $\sim 10^{-4}$ if the effective population size were equal to the observed census size. The colonizing population was parameterized such that $N_e = 183$, a finding consistent with N_e estimated in the BALB/c mice. The initial mutant allele frequency was set as 0.5 (1:1 ratio to the wild-type allele), and the mutant allele frequency was monitored for up to 8 days. Clearance rate ratios ranging from 0.952 to 1.053 were used for both the colonizing population and the ideal population. The simulation results indicated that selection was less efficient in the colonizing population than in the ideal population (Fig. 5). For example, when the clearance rate of the

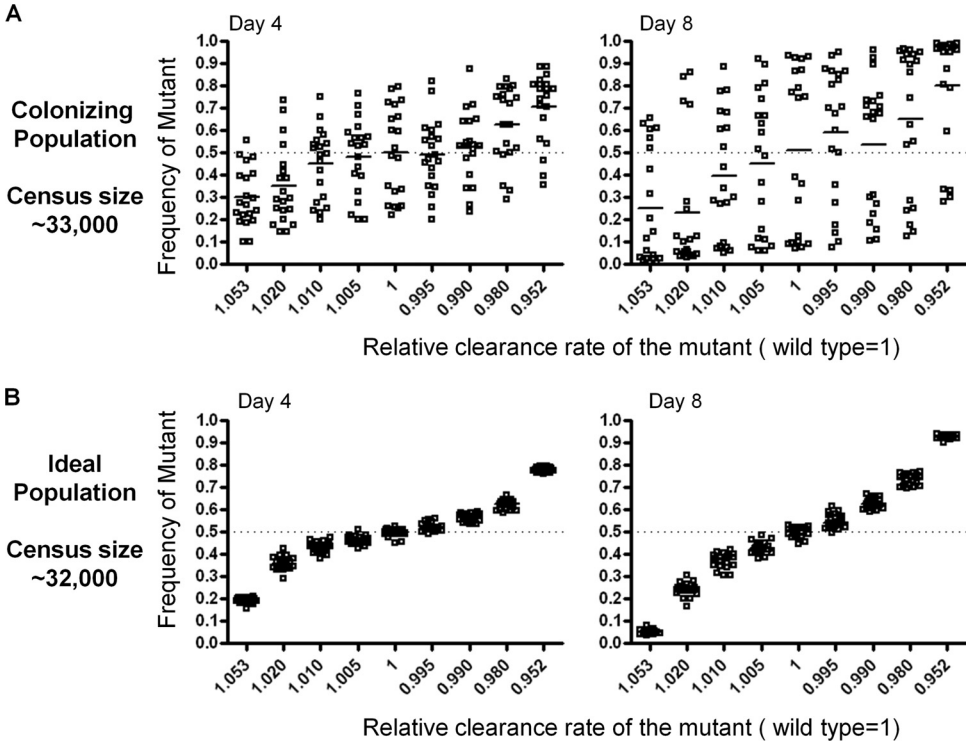

FIG 5 Effect of small N_e on the effectiveness of within-host selection. Simulations were performed based on a colonizing population model (A) or an ideal population model (B) (see Materials and Methods for details). A range of clearance rates were applied to the mutant allele, while the clearance rate for the wild-type allele was kept constant at 0.0043 min^{-1}. For each mutant clearance rate, 20 simulations were performed. The dotted lines indicate the initial frequency of the mutant allele (0.5 on day 0). Frequencies of the mutant alleles on day 4 (25 generations, left) and day 8 (50 generations, right) are shown. Bars represent means.

mutant allele was 0.990 that of the wild-type allele, mutant allele frequency increased above 0.5 in 13/20 simulations by day 4 in the colonizing population (Fig. 5A), while the mutant allele frequency increased above 0.5 in 20/20 simulations in the ideal population during the same period (Fig. 5C). By day 8, the mutant allele frequency showed a highly significant increase in the ideal population (mean increase = 0.1274, $n = 20$, $P < 0.0001$, one sample t test) (Fig. 5D). In the colonizing population, by contrast, the increase in mutant allele frequency was not statistically significant by day 8 (mean increase = 0.038, $n = 20$, $P = 0.57$, one sample Student t test) (Fig. 5B). Similar results were observed when the initial mutant allele frequency was set as 0.01 (see Fig. S1 in the supplemental material).

DISCUSSION

In this study, we estimated the effective population size of *Streptococcus pneumoniae* in a mouse colonization model by following the frequency change of two cocolonizing, competitively neutral pneumococcal strains. Since only allele frequency data on or after day 1 were used in N_e estimation, the effect of colonization bottleneck on frequency changes was minimized. In two mouse types, the N_e during nasal carriage was much smaller than the lower bound of census population that is estimated by the number of CFU recovered. The number of CFU recovered in the present study was smaller than the colonization density reported in other studies (9, 27–29), because at no time point did we intend to remove and recover the whole colonizing population. We purposely retrieved only a small fraction of the total population during live sampling in order to keep the colonization minimally disturbed. Even at the terminal sample, we did not exhaustively wash the mouse's upper respiratory tract but rather used a fixed recovery volume of 200 μl. Pneumococcal N_e also showed little temporal variation during colonization. We hypothesized that such a small N_e may reduce the effectiveness of within host selection for pneumococcus.

We constructed a mathematical model of colonization by considering two subpopulations of different growth dynamics that are established after a colonization bottleneck. In this model, a small, fast-replicating subpopulation generates most of the stochastic deviation in allele frequency that is then passed to a large subpopulation that is readily sampled but is not contributing much toward future generations. The model represents one, though not the only, biologically plausible mechanism that could generate such small effective population size. By simulation, we showed that this model could reproduce N_e patterns that were consistent with what was observed in mice experiments over a wide range of parameter values. A small N_e could be consistent with either a large or a small census population size (Fig. 4D), depending on the relative size of the two subpopulations. Thus, subpopulation structure, rather than the total population size, could be a critical determinant of N_e during pneumococcal colonization.

Using stochastic simulation of the model, we also examined the effectiveness of within-host selection for a mutant allele. Compared to an ideal population, the colonizing population showed two features: (i) the increase in frequency of a favorable allele was more variable and (ii) a favorable allele was less likely to become

fixed. These observations were consistent with strong genetic drift effects that interfered with the effectiveness of selection. In future investigations, it would be interesting to simultaneously estimate N_e and *in vivo* selection coefficient by using strains with medium and large fitness effects in competition experiments.

Our model certainly is not the only model that could produce the degree of stochastic variation observed. It is possible, for example, that there are more than two subpopulations with different contributions to successive generations. Alternatively, it is possible that the neutrally marked strains introduced in the experiment go on to mutate, and that some of these mutations (which occur at random with respect to the neutral marker) are advantageous in certain microanatomic sites within the nasopharynx. The consistency of results across experiments and the lack of positive correlation between frequency changes of neutral markers within a mouse over time make this selective explanation less likely. In any case, many models, including heterogeneous contributions to future generations or the presence of different selective microenvironments, which would produce random variation in neutral marker frequency as observed in our experiments, would also interfere with the action of selection to increase the frequency of, for example, a drug resistance mutation. It is for this reason that the concept of effective population size has been useful despite uncertainty about the precise mechanisms determining its value (10).

Studies of within-host competition between bacteria rarely comment on the aspects of stochasticity introduced by population bottlenecks and by a small effective population size. There are exceptions: transposon mutagenesis studies usually account for stochasticity, inexplicitly or explicitly, by focusing on strong and reproducible effects (8, 9), and there has been at least one deliberate experiment with neutrally marked, isogenic strains of enteric bacteria by Maskell and coworkers (30). Since N_e of pneumococcus during nasal colonization is likely to be 50- to 100-fold less than the carriage population, our model suggested that genetic drift may have a notable impact on the selection of pneumococcal variants, even those with substantial selection coefficients. The effects of genetic drift may help to explain the variation in estimated selection coefficients or competitive indexes often seen within an experiment; this is not a problem of noise introduced by the experimental technique but one of noise inherent in studying competition within a mouse. Nasopharyngeal swabs of humans (19) recover numbers of pneumococci similar to the numbers recovered by nasal wash in the present study (admittedly a comparison of limited interpretability, since neither technique quantifies the entire population present). If pneumococcal effective population sizes in humans are of comparable order to those in mice, then genetic drift may in some instances mask or overcome the effect of selection for resistant variants during treatment (31), selection against antimicrobial-resistant strains in the absence of treatment (1, 32), and selection for antigenic variation (3). This would be an interesting hypothesis for future investigation. It should be noted that the mouse is not a natural host for pneumococcal colonization, and more studies are needed to evaluate whether the small effective population size documented here applies to colonization in humans as native hosts.

The effect of small N_e is not limited to pneumococcal colonization. In a chicken model of colonization by *Campylobacter*, it was reported that the proportion of wild-type isogenic tagged strains present in chicken ceca after oral infection with a mixed population is not predictable from the inoculum (30). The unpredictability could be a result of both colonization bottleneck and a small N_e that increased the variability of the observed proportion. In addition, Grant et al. probed microbial population dynamics *in vivo* by simultaneously administering wild-type isogenic tagged strains of *Salmonella enterica* (33). By tracing the disappearance of strains through time, it was shown that independent bacterial subpopulations are established in different organs and that different bacterial populations mix between organs via the blood. Such population heterogeneity *in vivo* may also cause the effective population size of *Salmonella enterica* to be much smaller than the census population size and thus may influence the effectiveness of selection. Since the isogenic tagged strains allow tracking frequency change of multiple alleles simultaneously, data generated by this approach would be very informative to estimate the N_e of *Salmonella enterica in vivo*.

A small N_e could also affect the generation of new alleles. The probability that a neutral mutation occurs at a given position in an individual bacterium that is destined to contribute to future generations is approximated by the calculation $1 - e^{-N_e \mu t}$, where μ is the per nucleotide mutation rate and t is the number of generations. When N_e is much smaller than census population, it is possible that the rate of *de novo* mutagenesis in pneumococcus may be much slower than one would expect from the large census population.

ACKNOWLEDGMENTS

We thank Bernice Sim for technical assistance and Chris B. Ford at Harvard School of Public Health for technical assistance.

This study was supported in part by National Institutes of Health grant R01 AI048935 to M.L.

REFERENCES

1. **Trzcinski K, Thompson CM, Gilbey AM, Dowson CG, Lipsitch M.** 2006. Incremental increase in fitness cost with increased beta-lactam resistance in pneumococci evaluated by competition in an infant rat nasal colonization model. J. Infect. Dis. **193:**1296–1303.
2. **Lysenko ES, Lijek RS, Brown SP, Weiser JN.** 2010. Within-host competition drives selection for the capsule virulence determinant of *Streptococcus pneumoniae*. Curr. Biol. **20:**1222–1226.
3. **Li Y, Gierahn T, Thompson CM, Trzcinski K, Ford CB, Croucher N, Gouveia P, Flechtner JB, Malley R, Lipsitch M.** 2012. Distinct effects on diversifying selection by two mechanisms of immunity against *Streptococcus pneumoniae*. PLoS Pathog. **8:**e1002989. doi:10.1371/journal.ppat.1002989.
4. **Giraud A, Matic I, Tenaillon O, Clara A, Radman M, Fons M, Taddei F.** 2001. Costs and benefits of high mutation rates: adaptive evolution of bacteria in the mouse gut. Science **291:**2606–2608.
5. **Andisi VF, Hinojosa CA, de Jong A, Kuipers OP, Orihuela CJ, Bijlsma JJ.** 2012. Pneumococcal gene complex involved in resistance to extracellular oxidative stress. Infect. Immun. **80:**1037–1049.
6. **Cohen T, van Helden PD, Wilson D, Colijn C, McLaughlin MM, Abubakar I, Warren RM.** 2012. Mixed-strain *Mycobacterium tuberculosis* infections and the implications for tuberculosis treatment and control. Clin. Microbiol. Rev. **25:**708–719.
7. **Colijn C, Cohen T, Ganesh A, Murray M.** 2011. Spontaneous emergence of multiple drug resistance in tuberculosis before and during therapy. PLoS One **6:**e18327. doi:10.1371/journal.pone.0018327.
8. **Hensel M, Shea JE, Gleeson C, Jones MD, Dalton E, Holden DW.** 1995. Simultaneous identification of bacterial virulence genes by negative selection. Science **269:**400–403.
9. **van Opijnen T, Camilli A.** 2012. A fine scale phenotype-genotype virulence map of a bacterial pathogen. Genome Res. **22:**2541–2551.
10. **Charlesworth B.** 2009. Fundamental concepts in genetics: effective population size and patterns of molecular evolution and variation. Nat. Rev. Genet. **10:**195–205.
11. **Son MR, Shchepetov M, Adrian PV, Madhi SA, de Gouveia L, von**

Gottberg A, Klugman KP, Weiser JN, Dawid S. 2011. Conserved mutations in the pneumococcal bacteriocin transporter gene, *blpA*, result in a complex population consisting of producers and cheaters. mBio **2:**00179–11. doi:10.1128/mBio.00179-11.

12. **Davis KM, Akinbi HT, Standish AJ, Weiser JN.** 2008. Resistance to mucosal lysozyme compensates for the fitness deficit of peptidoglycan modifications by *Streptococcus pneumoniae*. PLoS Pathog. **4:**e1000241. doi:10.1371/journal.ppat.1000241.
13. **van Opijnen T, Camilli A.** 2012. A fine scale phenotype-genotype virulence map of a bacterial pathogen. Genome Res. doi:10.1101/gr.137430.112.
14. **Mastroeni P, Grant A, Restif O, Maskell D.** 2009. A dynamic view of the spread and intracellular distribution of *Salmonella enterica*. Nat. Rev. Microbiol. **7:**73–80.
15. **Giraud A, Fons M, Taddei F.** 2003. Impact of mutation rate on the adaptation of gut bacteria. J. Soc. Biol. **197:**389–396. (In French.)
16. **Briles DE, Novak L, Hotomi M, van Ginkel FW, King J.** 2005. Nasal colonization with *Streptococcus pneumoniae* includes subpopulations of surface and invasive pneumococci. Infect. Immun. **73:**6945–6951.
17. **Bogaert D, De Groot R, Hermans PW.** 2004. *Streptococcus pneumoniae* colonisation: the key to pneumococcal disease. Lancet Infect. Dis. **4:**144–154.
18. **Simell B, Auranen K, Kayhty H, Goldblatt D, Dagan R, O'Brien KL, Pneumococcal Carriage Group.** 2012. The fundamental link between pneumococcal carriage and disease. Expert Rev. Vaccines **11:**841–855.
19. **Albrich WC, Madhi SA, Adrian PV, van Niekerk N, Mareletsi T, Cutland C, Wong M, Khoosal M, Karstaedt A, Zhao P, Deatly A, Sidhu M, Jansen KU, Klugman KP.** 2012. Use of a rapid test of pneumococcal colonization density to diagnose pneumococcal pneumonia. Clin. Infect. Dis. **54:**601–609.
20. **Wang J.** 2003. Maximum-likelihood estimation of admixture proportions from genetic data. Genetics **164:**747–765.
21. **Wang J.** 2001. A pseudo-likelihood method for estimating effective population size from temporally spaced samples. Genet. Res. **78:**243–257.
22. **Williamson EG, Slatkin M.** 1999. Using maximum likelihood to estimate population size from temporal changes in allele frequencies. Genetics **152:**755–761.
23. **Balaban NQ, Merrin J, Chait R, Kowalik L, Leibler S.** 2004. Bacterial persistence as a phenotypic switch. Science **305:**1622–1625.
24. **Cao Y, Gillespie DT, Petzold LR.** 2007. Adaptive explicit-implicit tau-leaping method with automatic tau selection. J. Chem. Physics **126:**224101.
25. **Wang J, Whitlock MC.** 2003. Estimating effective population size and migration rates from genetic samples over space and time. Genetics **163:**429–446.
26. **Hathaway LJ, Brugger SD, Morand B, Bangert M, Rotzetter JU, Hauser C, Graber WA, Gore S, Kadioglu A, Muhlemann K.** 2012. Capsule type of *Streptococcus pneumoniae* determines growth phenotype. PLoS Pathog. **8:**e1002574. doi:10.1371/journal.ppat.1002574.
27. **Rosch JW, Mann B, Thornton J, Sublett J, Tuomanen E.** 2008. Convergence of regulatory networks on the pilus locus of *Streptococcus pneumoniae*. Infect. Immun. **76:**3187–3196.
28. **Cron LE, Bootsma HJ, Noske N, Burghout P, Hammerschmidt S, Hermans PW.** 2009. Surface-associated lipoprotein PpmA of *Streptococcus pneumoniae* is involved in colonization in a strain-specific manner. Microbiology **155:**2401–2410.
29. **Cron LE, Stol K, Burghout P, van Selm S, Simonetti ER, Bootsma HJ, Hermans PW.** 2011. Two DHH subfamily 1 proteins contribute to pneumococcal virulence and confer protection against pneumococcal disease. Infect. Immun. **79:**3697–3710.
30. **Coward C, van Diemen PM, Conlan AJ, Gog JR, Stevens MP, Jones MA, Maskell DJ.** 2008. Competing isogenic *Campylobacter* strains exhibit variable population structures in vivo. Appl. Environ. Microbiol. **74:**3857–3867.
31. **Anderson KB, Tan JS, File TM, Jr, DiPersio JR, Willey BM, Low DE.** 2003. Emergence of levofloxacin-resistant pneumococci in immunocompromised adults after therapy for community-acquired pneumonia. Clin. Infect. Dis. **37:**376–381.
32. **Andersson DI, Hughes D.** 2010. Antibiotic resistance and its cost: is it possible to reverse resistance? Nat. Rev. Microbiol. **8:**260–271.
33. **Grant AJ, Restif O, McKinley TJ, Sheppard M, Maskell DJ, Mastroeni P.** 2008. Modeling within-host spatiotemporal dynamics of invasive bacterial disease. PLoS Biol. **6:**e74. doi:10.1371/journal.pbio.0060074.